Received: 4 December 2019 | Revised: 1 April 2020 | Accepted: 13 July 2020

DOI: 10.1002/bit.27514

ARTICLE

BIOTECHNOLOGY BIOENGINEERING WILEY

Improving the analytical toolbox to investigate copurifying host cell proteins presence: *N*-(4)-(β-acetylglucosaminyl)-L-asparaginase case study

Séverine Clavier[1] | Delphine Fougeron[1] | Suzana Petrovic[1] | Hagit Elmaleh[1] | Céline Fourneaux[1] | Dawid Bugnazet[1] | Francis Duffieux[2] | Alessandro Masiero[3] | Shibani Mitra-Kaushik[4] | Bruno Genet[1] | Yann Fromentin[1] | Patrick Kreiss[1] | Bénédicte Laborderie[1] | Dominique Brault[1] | Jean-Michel Menet[1]

[1]BioAnalytics, Biologics Development, Sanofi R&D, Vitry-Sur-Seine, France

[2]Protein Science and Technology, Biologics Research, Sanofi R&D, Vitry-Sur-Seine, France

[3]e-Biology, Biologics Research, Sanofi R&D, Vitry-Sur-Seine, France

[4]BioAnalytics, Biologics Development, Sanofi R&D, Framingham, Massachusetts

Correspondence
Séverine Clavier, BioAnalytics, Biologics Development, Sanofi R&D, 13, quai Jules Guesde, Vitry-Sur-Seine 94400, France.
Email: severine.clavier@sanofi.com

Abstract

Levels of host cell proteins (HCPs) in purification intermediates and drug substances (DS) of monoclonal antibodies (mAbs) must be carefully monitored for the production of safe and efficacious biotherapeutics. During the development of mAb1, an immunoglobulin G1 product, unexpected results generated with HCP Enzyme-Linked Immunosorbent Assay (ELISA) kit triggered an investigation which led to the identification of a copurifying HCP called *N*-(4)-(β-acetylglucosaminyl)-L-asparaginase (AGA, EC3.5.1.26) by liquid chromatography–tandem mass spectrometry (LC-MS/MS). The risk assessment performed indicated a low immunogenicity risk for the copurifying HCP and an ad hoc stability study demonstrated no mAb glycan cleavage and thus no impact on product quality. Fractionation studies performed on polishing steps revealed that AGA was coeluted with the mAb. Very interestingly, the native digestion protocol implemented to go deeper in the MS–HCP profiling was found to be incompatible with correct AGA detection in last purification intermediate and DS, further suggesting a hitchhiking behavior of AGA. In silico surface characterization of AGA also supports this hypothesis. Finally, the combined support of HCP ELISA results and MS allowed process optimization and removal of this copurifying HCP.

KEYWORDS

HCP ELISA assay, HCP identification and quantitation by LC–MS/MS, hitchhiking behavior, host cell proteins, *N*-(4)-(β-acetylglucosaminyl)-L-asparaginase, risk assessment

1 | INTRODUCTION

Monoclonal antibodies (mAbs) are biotherapeutic products that can achieve outstanding success in treating many life-threatening and chronic diseases. mAbs are commonly produced within chinese hamster ovary (CHO) cells supernatant along with host cell proteins (HCPs). One of the downstream process (DSP) primary goals is HCP elimination performed using a series of chromatographic steps often

starting with a capture step and typically followed by one or more polishing steps. It is crucial to carefully monitor residual HCP as some of them can impact mAb's quality or its formulation components due to their enzymatic activity. For instance, the intracellular enzyme thioredoxin was shown to induce the reduction of disulfide bonds in harvested cell culture fluids (Koterba, Borgschulte, & Laird, 2012). CHO lipases (LPLA2 and PLBL2) were discussed to be responsible for polysorbates degradation resulting in the formation of particles during long-term storage (Dixit, Salamat-Miller, Salinas, Taylor, & Basu, 2016; Hall, Sandefur, Frye, Tuley, & Huang, 2016). Similarly, particle formation during storage was attributed to the proteolytic activity of cathepsin D at very low levels (Bee et al., 2015).

Furthermore, HCP may also have an impact on patient safety due to their biological activity or immunogenicity (Gutiérrez, Moise, & Groot, 2012). Indeed, hamster proteins can be detected as exogenous in mAb-treated patients and trigger immune responses with the production of anti-HCP antibodies but also of antidrug antibodies through the adjuvant effect of HCP (Bracewell, Francis, & Smales, 2015). Examples of impurities responsible for adverse events, like MCP-1 causing unwanted histamine release, flagellin stimulating Toll-like receptor, or PLBL2 leading to the production of anti-PLBL2 antibodies, have been recently gathered in one publication (Vanderlaan et al., 2018). Thus, it is particularly important to perform an appropriate risk assessment to determine whether actions have to be implemented to secure biotherapeutic project development.

The level of residual HCP is a critical quality attribute (CQA) and is monitored by HCP enzyme-linked immunosorbent assays (ELISA) as in-process monitoring (IPM) as well as drug substance (DS) release tests. The detection of multiple HCP species is based on polyclonal ELISA reagents generated by immunization with representative HCP antigens. HCP ELISA assays are, thus, inherently "immunologically weighted" with the most immunogenic species being readily detected and a risk of having weakly or nonimmunogenic proteins poorly detected. Moreover, the polyclonal nature of this ELISA may lead to a well-known issue where nondilutional linearity induces inconsistent quantitation of HCP. This behavior is observed when one or several specific HCP is/are more abundant than corresponding coating/detection ELISA antibodies. In this case, it is recommended to perform several dilutions of a given sample (USP 39 NF 34, General Chapter <1132> Residual Host Cell Protein Measurement in Biopharmaceuticals).

Over the past few years, the use of mass spectrometry (MS) as an orthogonal method to HCP ELISA assays has grown rapidly (Wang, Hunter, & Mozier, 2009; Zhu-Shimoni et al., 2014). While HCP ELISA assays quantify the total amount of HCP in a sample, MS allows identifying and quantifying individual HCP and has, thus, become a key tool in understanding HCP ELISA results. However, the identification of HCP in purified mAb samples is challenging due to their low abundance. Therefore, sample preparation methods based on biotherapeutic depletion have been developed to gain sensitivity (Huang et al., 2017).

Here, we describe a case study in which routinely used HCP ELISA raised an alert by detecting an unexpected HCP level increase at several steps of the purification process and in the DS. Liquid chromatography-tandem mass spectrometry (LC–MS/MS) was used as an investigation tool to ascertain the results and provided the identification of a single copurifying HCP, *N*-(4)-(β-acetylglucosaminyl)-L-asparaginase (AGA). This triggered a risk assessment to ensure patient safety and product stability. Furthermore, thorough analytical and characterization studies were performed to improve this HCP quantitation but also to better understand its interaction with the mAb. Finally, these results supported the successful purification process optimization and AGA removal.

2 | MATERIALS AND METHODS

2.1 | Total HCP quantitation by ELISA

Total HCP quantitation is routinely performed using an in-house ELISA (hereafter named HCP ELISA). Polyclonal antibodies were produced by immunizing goats with representative mock supernatant. Anti-HCP antibodies were purified by protein G followed by antigen affinity purification and coated on the plate before the addition of mAb1 samples (purification intermediates or DS) and secondary antibodies conjugated to horseradish peroxidase (HRP). After 2-hr incubation, plates were washed with TBS-Tween. HRP substrate (tetramethylbenzidine) was then added to the plates for 30 min before the acidic solution was used to stop the reaction. Optical densities were read at 450 nm on a spectrophotometer. Standard curves and concentrations of unknown samples were determined using a four-parameter logistic curve.

2.2 | Tryptic digestion in denaturing conditions

After concentration and desalting, mAb1 samples were denatured using RapiGest® (Waters). Samples were subsequently reduced with dithiothreitol (DTT), alkylated with iodoacetamide, and digested overnight at 37°C with trypsin:mAb1 ratio of 1:100. After digestion, Rapigest® was precipitated by adding HCl and pelleted by centrifugation. The supernatant was collected, diluted 10-fold, and 1 µg of mAb digest was injected.

2.3 | Tryptic digestion in native conditions

After desalting and concentration mAb1 purification intermediates were submitted to tryptic digestion, overnight at 37°C with trypsin:-mAb1 ratio of 1:400 in Tris-HCl 50 mM pH 8 buffer. Samples were then reduced with DTT and heated 10 min at 90°C. After centrifugation, the supernatant was collected and 2.5 µl of digest were injected for each sample corresponding to an initial mAb amount of 10 µg.

2.4 | HCP profiling by nanoLC–MS/MS

Tryptic peptides were separated on an Acclaim Pepmap 75 µm × 50 cm 3-µm 100-Å reverse phase C_{18} column installed on an

Ultimate 3000 NanoLC system (Dionex) coupled to a Q-Exactive Plus MS (Thermo Fisher Scientific). MS and MS/MS data were acquired using a top 10 data-dependent acquisition mode with Xcalibur 4.0 software. Data obtained were searched using the Mascot search engine against the Uniprot CHO database.

2.5 | AGA absolute quantitation

Synthetic heavy-labeled peptides ($^{15}N^{13}C$ C-terminal lysine or arginine) SLHSEWASK and NC(CAM)QPNFWR were ordered as 1 mg lyophilized powder from Pepscan (Lelystad, The Netherlands). They were resuspended in water/acetonitrile/formic acid and spiked at a concentration of 100 ppm (=100 ng AGA/mg mAb1) in mAb digests. One microgram of digests was analyzed using the NanoLC–MS/MS system described in the previous paragraph. Data were acquired in triplicates using the parallel reaction monitoring (PRM) mode targeting charge 2+ ions of light- and heavy-labeled versions of SLHSEWASK and NC(CAM)QPNFWR peptides. Data were retreated using Skyline v4.1.0.11796 open-source software (University of Washington) using the most intense transition of each peptide for quantitation.

2.6 | Immunogenicity in silico risk assessment

Three publically available sequences of AGA (*Cricetulus griseus*: strain K1 Genbank ID EGV92246, strain 17A/GY Genbank ID ERE87799, and Homo sapiens: Genbank ID P20933) were aligned using NCBI COBALT alignment tool to evaluate homology and sequence identity. Using the EpiMatrix in silico major-histocompatibility complex (MHC)-peptide binding prediction algorithm, the amino acid sequence of the HCP was screened for the presence of putative T cell epitopes restricted by human leucocyte antigen (HLA) class II. By aggregating the EpiMatrix scores of the putative epitopes identified in the analysis, and relative risk as compared to the CHO proteome, an overall HCP specific EpiMatrix protein score was calculated (Bailey-Kellogg et al., 2014). Finally, using an orthogonal algorithm, immune epitope database (IEDB), an analysis of peptide binding to MHC class II alleles was performed. The IEDB algorithm divided the amino acid sequence into all possible 15-mer peptides and then predicted the ability of each to bind to a set of 27 common MHC class II alleles which covered >99% of the population.

2.7 | Homology modeling, structural evaluation, and hydrophobicity in silico characterization

A homology model of AGA was built by means of Discovery Studio Suite 2017, using the human ortholog structure (Protein Data Bank ID: 1APZ [Oinonen, Tikkanen, Rouvinen, & Peltonen, 1995]). The sequence identity was 79.3% and sequence similarity was 90.7%. Surface hydrophobicity was calculated by means of spatial aggregation propensity algorithm (Chennamsetty, Voynov, Kayser, Helk, & Trout, 2010).

2.8 | Recombinant protein production and characterization

The coding sequence of AGA from *Cricetulus griseus* was retrieved from the UniProt database (accession number: G3HGM6_CRIGR). According to its annotation and the sequences alignments, the signal peptide was annotated from positions M1 to G24 and the proprotein from positions F25 to I346. Therefore, an expression cassette was designed in which a polyhistidine tag (His6) and a tobacco etch virus (TEV) protease site were introduced between the signal peptide and the proprotein sequence. The resulting construct sequence (SP-His6-TEV-AGA-F25-I346) was optimized for human codon usage and synthesized (GeneArt). This expression cassette was subcloned into a mammalian expression vector for transient transfection into the HEK293FS cell line (Thermo Fisher Scientific). After 7 days post-transfection, the recombinant AGA (recAGA) was purified from the clarified supernatant by immobilized metal affinity chromatography (IMAC) on a Ni-Sepharose column (GE Healthcare). Fractions enriched in recAGA were dialyzed overnight in Dulbecco's phosphate-buffered saline buffer at 4°C in presence of 2% (wt/wt) of His-tagged TEV protease to cleave off the *N*-terminal polyhistidine tag. His-tagged TEV protease and His-tag were removed by a negative IMAC and the tag-less recAGA was applied on a Superdex 75 pg column (GE Healthcare). The recAGA was eluted as a single peak and was further concentrated up to 2.30 mg/ml before storage at 2–8°C.

The purified recAGA was characterized by LC–MS and sodium dodecyl sulfate-polyacrylamide gel electrophoresis (SDS-PAGE) in reducing condition with or without prior *N*-deglycosylation overnight with PNGase (New England Biolabs) at 37°C. Five micrograms of only reduced recAGA and 5 µg of reduced *N*-deglycosylated recAGA were migrated on a 12% Tris-glycine SDS-PAGE and colored by GelCode Blue Stain for 1 hr. Intact *N*-deglycosylated LC–MS analysis was performed on an Exion ultra-performance liquid chromatography coupled to an X500-B quadrupole time-of-flight MS (Sciex). recAGA of 0.2 µg were separated on a MAbPac Reverse Phase 4 µm 2.1 × 50 mm column. Data were acquired and summed mass spectra were reconstructed with Sciex OS software. GPMAW 9.51 was used to perform mass calculations and help manual assignment of masses observed.

2.9 | Polishing steps fractionation studies

A peak fractionation study was carried out on the first polishing step. A representative material (post capture step) was loaded on the lab-scale column. mAb1 was bound to the column and the unbound material was washed (four column volumes). Elution was then initiated and the collection was monitored following UV signal (>500 mAu). The column was sanitized using sodium hydroxide 0.1 N.

Approximately 30 fractions were collected from the load to sanitization steps. For fractions collected during sanitization, a buffer exchange was applied to eliminate sodium hydroxide and maintain protein integrity. Samples collected were analyzed by HCP ELISA and several fractions were also characterized by LC–MS/MS without any prior dilution or concentration steps to keep the information on the relative abondance of AGA. Peak fractionation study was also performed on the second polishing step (flow-through chromatography). Fifteen fractions were collected and analyzed by HCP ELISA.

3 | RESULTS AND DISCUSSION

3.1 | Unexpected HCP increase and linearity assessment

3.1.1 | Raising the alert

HCP ELISA raised an alert by measuring significantly higher HCP values for polishing steps and DS samples of mAb1, and IgG1 product. Indeed, as illustrated in Figure 1, while the post capture step results showed no significant variations, results were greater than the mean ± 3σ on Batch O for the second polishing step. This increase was confirmed on the following batches on both polishing steps and DS and triggered an investigation.

3.1.2 | Dilutional linearity assessment

Samples from polishing steps and DS were diluted initially to their respective minimum required dilution, where spike recovery had been previously confirmed, and then twofold serially diluted to below the assay's limit of quantitation (LoQ; 5 ng/ml). To evaluate the assay linearity, Guide 1 of the USP1132 was followed: all values within 20–25% of the maximum HCP value above the LoQ were averaged.

Dilutional linearity was compared for batches processed before (Batch B) and after (Batch O) the HCP levels increase was observed. The linearity behavior was significantly different for the two batches: Batch O showed a significantly higher amount of HCP and nonlinear behavior, which was not previously encountered (Figure 2). These observations were confirmed on both polishing steps and DS samples on Batch O as well as on the following batches. This suggests an antigen excess compared to the available antibodies in the HCP ELISA, that is, present in the abundance of one or more HCP from Batch O onwards. HCP identification was, therefore, necessary to understand whether the newly observed nonlinearity behavior was due to an increased level of HCP already present in previous batches or to a new HCP population.

3.2 | HCP identification and quantitation by LC–MS/MS

3.2.1 | Establishing HCP profiles along with DSP steps

To identify HCP(s) responsible for this increase, purification intermediates and DS for batches produced either before or after the HCP levels change were digested in denaturing conditions and analyzed by LC–MS/MS. HCP profiles were found to be very similar in all post capture step samples, consistent with HCP ELISA results, with up to nine HCP confidently identified (Table 1).

For post first and second polishing steps, only one HCP, AGA, was systematically identified both before and after the HCP level increase. However, for DS samples, AGA was identified only from Batch O onwards. As for previous batches, B, J, and N, it was possible to retrospectively detect peptide ions corresponding to this HCP in DS samples but these MS signals were too low to allow identification based on MS/MS spectra. This emphasizes the challenge of low-levels-residual HCP detection even with the most sensitive instruments currently available. These results indicated that the increase

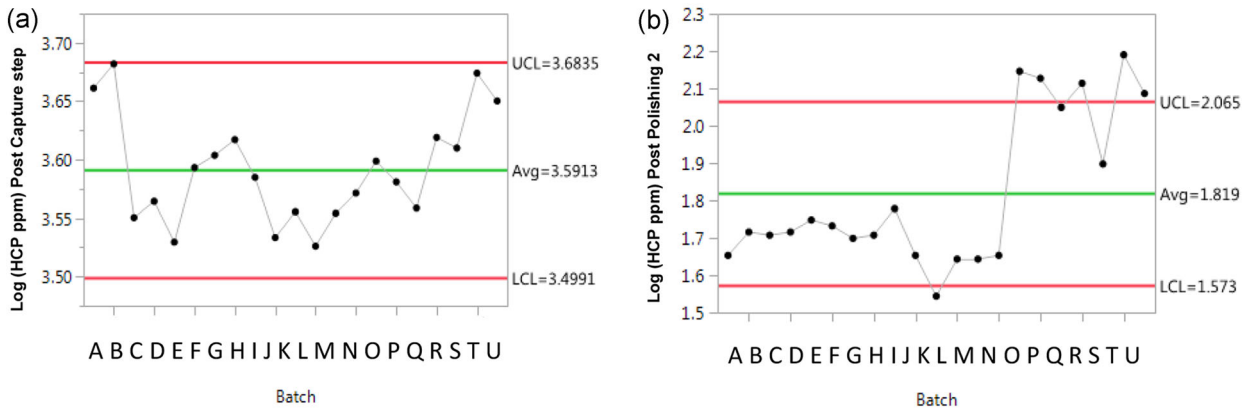

FIGURE 1 Trending of the total host cell protein (HCP) content quantified by HCP enzyme-linked immunosorbent assay at the (a) post capture step and (b) post second polishing step. Avg, average; LCL, lower control limit; UCL, upper control limit [Color figure can be viewed at wileyonlinelibrary.com]

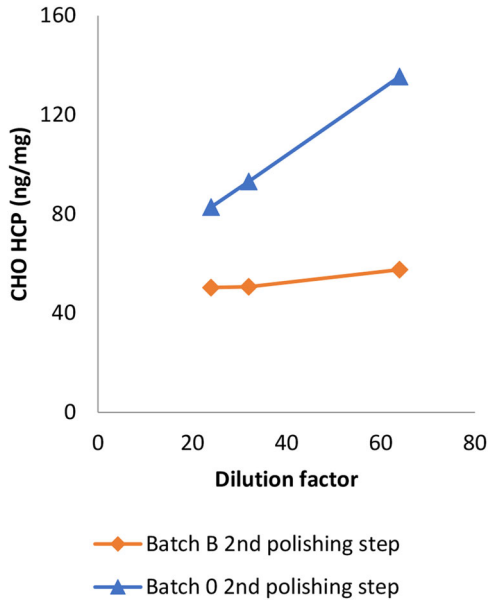

FIGURE 2 Dilution linearity assessment at the second polishing step for a batch before (Batch B) and a batch after (Batch O) the increase of total HCP content. Twofold dilution series performed using the HCP ELISA assay until the assay LoQ was reached. CHO, Chinese hamster ovary; ELISA, enzyme-linked immunosorbent assay; HCP, host cell protein; LoQ, limit of quantitation [Color figure can be viewed at wileyonlinelibrary.com]

observed by HCP ELISA was not due to new HCP but to a decrease in clearance efficiency of one given HCP: AGA.

AGA was identified by matching with the UniProt/TrEMBL *Cricetulus griseus* database accession entry G3HGM6. This protein of 346 amino acids has a molecular weight of 37.27 kDa. As there is no literature available for this protein in CHO cells, information for human and mice homolog proteins was gathered. AGA enzyme is synthesized as a precursor polypeptide which is activated in the endoplasmic reticulum by a signal proteolytic cleavage step resulting in two subunits, an α and a β chains (Ikonen, Julkunen, Tollersrud, Kalkkinen, & Peltonen, 1993). The two subunits associate into a dimeric enzyme molecule by noncovalent interactions and, upon entry into lysosomes, the α-subunit is further processed to eliminate an α-propeptide (Ikonen et al., 1991; Figure 3).

To determine the maturation state of AGA, tryptic peptide ions corresponding to the cleavage domain and α-chain propeptide were examined. TIGMVVIHK peptide corresponding to the *N*-terminal tryptic peptide of the β-chain was identified as well as YCGPYKPSGSLEWAISAHK and QVDIHNHD peptides corresponding to the α-chain + propeptide (data not shown). In contrast, YCGPYKPSG peptide corresponding to the fully matured α-chain and QVDIHNHDTIGMVVIHK corresponding to the AGA proenzyme form was not detected (data not shown). These observations indicated that AGA had started its maturation process with the cleavage into two subunits but with no evidence that the process was completed and the enzyme functional.

3.2.2 | Absolute quantitation of AGA

On the basis of tryptic peptides identified by LC–MS/MS, SLHSEWASK and NC(CAM)QPNFWR were chosen as surrogate peptides to perform absolute quantitation of AGA on purification intermediates of four batches, two produced before and two after the HCP increase (Figure 4).

Post capture step, HCP ELISA results were in the range of 3,500–4,500 ppm corresponding to at least nine HCP identified (Table 1). Quantitation of AGA by PRM–MS indicated that its

TABLE 1 Summary of HCP identified by NanoLC–MS/MS for post capture step, post first and second polishing steps for all batches (coloration of the cells in green indicates that the host cell protein was identified)

Identified Proteins	Post capture step	Post 1st polishing step	Post 2nd polishing step
Basement membrane-specific heparan sulfate proteoglycan core protein			
Semaphorin-3B			
N(4)-(Beta-N-acetylglucosaminyl)-L-asparaginase			
Tubulointerstitial nephritis antigen-like			
Peroxidasin-like			
Clusterin			

Abbreviations: HCP, host cell protein; LC–MS/MS, liquid chromatography–tandem mass spectrometry.

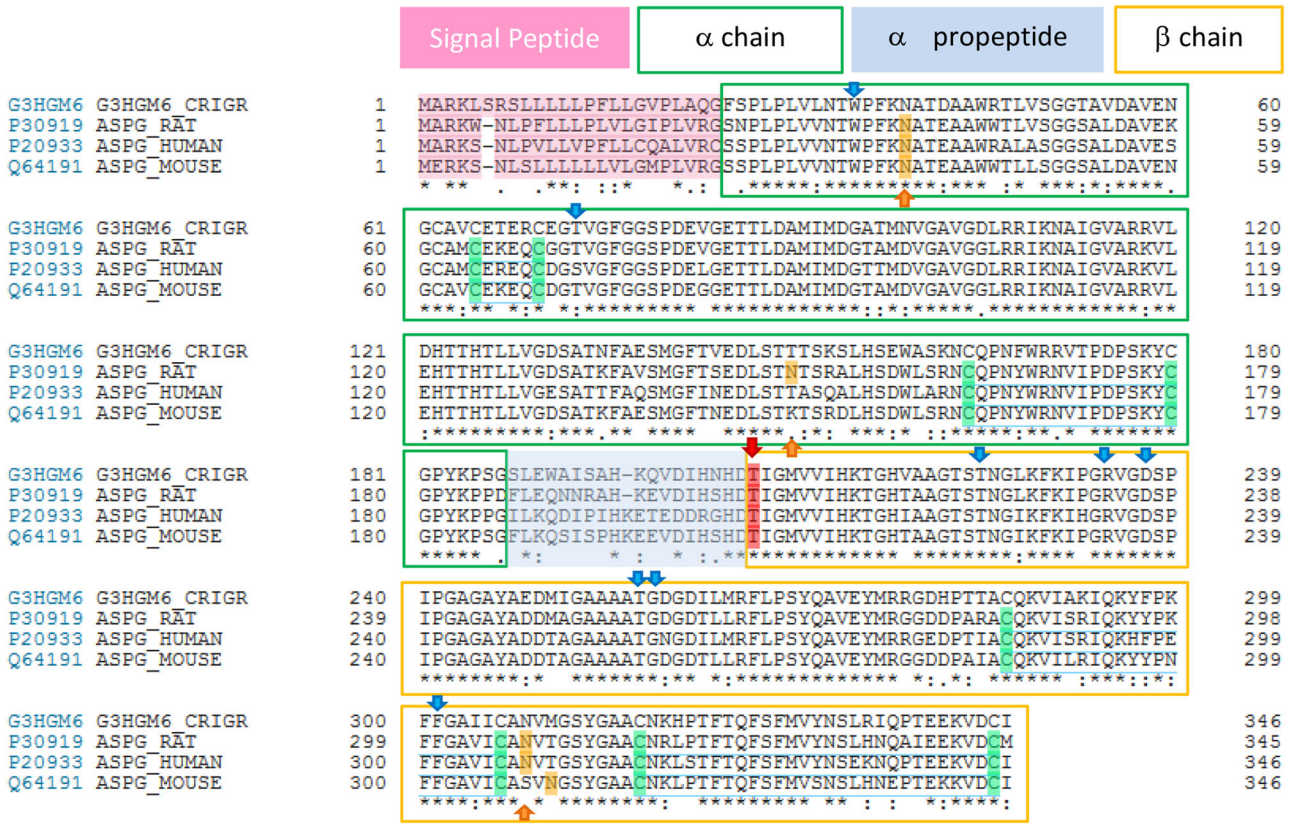

FIGURE 3 Sequence alignment and annotation of human, rat, mouse, and hamster *N*-(4)-(β-acetylglucosaminyl)-L-asparaginase. Cysteines involved in disulfide bond highlighted in green, *N*-glycosylation sites designated with an orange arrow, residues of the active site highlighted by a blue arrow, and conserved nucleophile residue colored in red [Color figure can be viewed at wileyonlinelibrary.com]

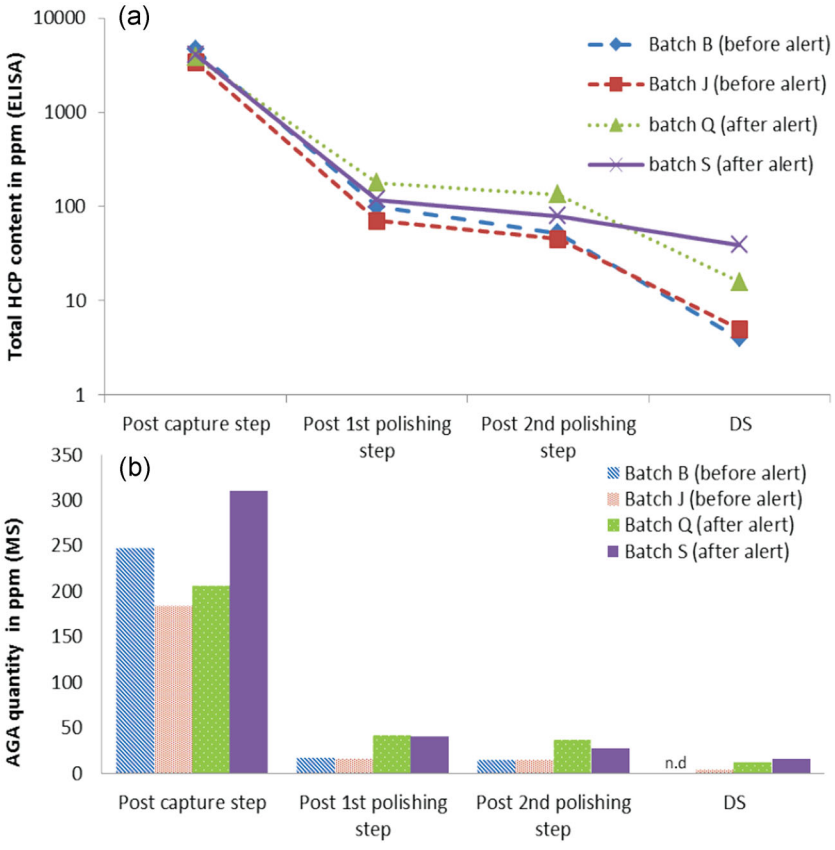

FIGURE 4 HCP clearance during the downstream purification process. (a) Total HCP content in ppm measured by HCP ELISA. (b) Absolute targeted quantitation of AGA for four batches, two before and two after the HCP alert. AGA, *N*-(4)-(β-acetylglucosaminyl)-L-asparaginase; DS, drug substance; ELISA, enzyme-linked immunosorbent assay; HCP, host cell protein; nd, not detected; ppm, parts per million [Color figure can be viewed at wileyonlinelibrary.com]

contribution was around 200–300 ppm. MS results confirmed the absence of trend for this step as observed by HCP ELISA (Figure 1).

Post first and second polishing steps, the only HCP identified by MS was AGA. Quantitation by PRM–MS showed a significant clearance of AGA content post first polishing step for all batches. However, AGA residual quantities were significantly lower for Batches B and J compared to Batches Q and S, indicating a clearance loss at the first polishing step (Figure 4). This was consistent with HCP ELISA results, confirming that higher HCP ELISA values observed at post first polishing step from Batch O were, thus, linked with increased levels of AGA. While a slight decrease of total HCP content was seen between the first and second polishing step, AGA amounts quantified by MS were comparable. To ensure that this minor difference was not due to unidentified HCP, another sample preparation method was tested (see Section 3.6) and MS/MS data were searched with a larger database without specifying the taxonomy but did not lead to any further identification (data not shown). In the DS, both total HCP content determined by HCP ELISA and AGA amounts quantified by MS were slightly lower compared to the second polishing step.

3.3 | recAGA: Production and use thereof

3.3.1 | recAGA protein production and characterization

A batch of recAGA hamster protein was produced and characterized by LC–MS and SDS-PAGE. LC–MS analysis of the *N*-deglycosylated protein allowed detecting one species with a molecular weight of 15,162 kDa corresponding to the β chain and several additional species between 18,256 and 19,551 kDa corresponding to the α-chain associated either with the full-length α-propeptide or with partially processed α-propeptides (Figure S1a) also visible on the SDS-PAGE (Figure S1b). The α-chain alone corresponding to the fully matured AGA protein was not identified suggesting that recAGA was not enzymatically active.

3.3.2 | HCP ELISA Kit ability to detect AGA

Several known concentrations of recAGA were tested in the HCP ELISA assay. Results showed recoveries close to 100% for very low level of recAGA (<10 ng/ml; Figure 5a). With the increase of recAGA amount, the recoveries tend to decrease with the observation of a plateau at about 10 ng/ml. These results were consistent with the observation of nonlinear behavior in samples containing AGA at >10 ng/ml per ELISA well and could also explain the satisfying linearity observed on samples with less AGA content before Batch O.

In parallel, a commercial generic CHO–HCP ELISA assay was also tested with the same levels of recAGA (Figure 5b). The results showed a twofold lower quantitation of this HCP with the generic assay in comparison with the in-house one. Moreover, two available commercial ELISA assays for specific AGA quantitation targeting hamster species were also tested but both showed an absence of response for all tested samples due to a significant matrix effect (data not shown). Additional dilutions were tested to overcome the matrix effect, but samples were then too diluted to be within the assay's range. Of note, these assays were not designed for cell culture supernatant and cell lysate samples, but for hamster biological fluids or tissue which may explain results observed. Consequently, the in-house total HCP ELISA assay remains the best available ELISA assay for total HCP quantitation in the dilution linearity range demonstrated.

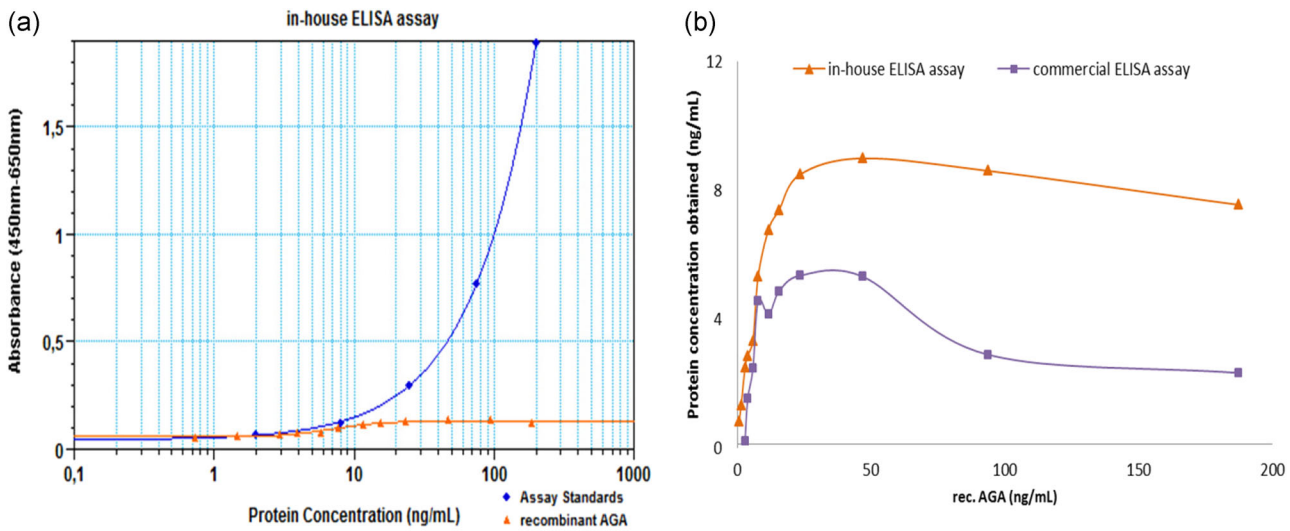

FIGURE 5 Known levels of recombinant AGA tested in the HCP ELISA assay (a) and comparison of recombinant AGA (recAGA) quantitation between the in-house HCP ELISA and a commercial assay (b). AGA, *N*-(4)-(β-acetylglucosaminyl)-L-asparaginase; ELISA, enzyme-linked immunosorbent assay; HCP, host cell protein [Color figure can be viewed at wileyonlinelibrary.com]

3.4 | Risk assessment

3.4.1 | Risk assessment: Product risk

AGA is a lysosomal amidase, thermostable, and enzymatically active at 37°C (McGovern, Aula, & Desnick, 1983) that catalyzes one of the final steps in the glycoproteins' breakdown (Makino, Kojima, & Yamashina, 1966). The enzyme cleaves the bond between Asparagine (Asn) residues and *N*-acetylglucosamine, and has a substrate specificity that required both a free α-carboxyl and free α-amino group on the Asn (Aronson & Kuranda, 1989; Tikkanen, Riikonen, Oinonen, Rouvinen, & Peltonen, 1996). Although an absence of AGA activity was also reported on fucosylated glycoasparagines (Aronson & Kuranda, 1989), a stability study was designed to assess the potential impact on the product and most specifically the absence of mAb1 *N*-glycan cleavage. A DS batch containing a low HCP level (Batch N, 5 ppm of HCP) and a batch containing a high HCP level (Batch R, 40 ppm of HCP) were submitted to an accelerated thermal stress of 1 month at 40°C. Among mAb1 CQAs, the glycosylation profile (focusing on afucosylation) was followed using hydrophilic-interaction liquid chromatography fluorescence and aglycosylation level was measured by reduced capillary Gel Electrophoresis (cGE) (nonglycosylated heavy-chain quantitation). Furthermore, as it has been shown that a decrease in core-fucose levels leads to a pronounced increase in antibody-dependent cell cytotoxicity (Okazaki et al., 2004), this biological activity was followed. Results obtained indicated that CQA potentially impacted did not vary as a function of AGA level in the product under thermal stress conditions, thus AGA did not appear to jeopardize mAb1 quality (Table S1).

3.4.2 | Risk assessment: Patient risk

EpiMatrix scores for AGA were plotted on an immunogenicity potential scale comparing the risk for this HCP to other therapeutic proteins and mAbs (Figure S2). The EpiMatrix score of the input AGA sequence is −11.79 indicating a low immunogenic potential. Of the 53 peptides which could potentially bind at least one HLA allele, 33 were found to be homologous to the human genome and 20 were CHO specific. None of the peptides within AGA were identified as an HCP immunogen in the published literature or public domain.

To confirm the outcome of the EpiMatrix HCP assessment, an orthogonal in silico analysis of the amino acid sequence was performed using the IEDB algorithm. However, most of the HLA binding sequences were either identical to human AGA or predicted to bind to only one or two of the common well-documented HLA alleles. Of note, AGA is also a relatively small protein (348 amino acids) in comparison with other CHO proteins which probably accounts for this lower epitope content. Taken together both approaches suggest low immunogenic risk for AGA.

3.5 | In-depth understanding of HCP clearance during polishing steps

Peak fractionation studies were performed on the first and second polishing steps to track product (high and low molecular weight species) and process (residual HCP and DNA) related impurities removal. Hereafter, only HCP results were presented.

HCP content was mapped through the first polishing step consecutive phases including load, wash, elution, and sanitization. mAb1 elution profile was monitored by UV280, associated with ELISA HCP quantitation and LC–MS/MS profiling performed on some selected fractions (Figure 6a). While HCP ELISA content in fractions collected during the load step was below the limits of detection, most HCP were detected during the wash step. On the contrary, AGA was mainly identified during mAb1 elution where it was four times more abundant than in the wash fractions. Finally, several HCPs were recovered in the sanitization fractions.

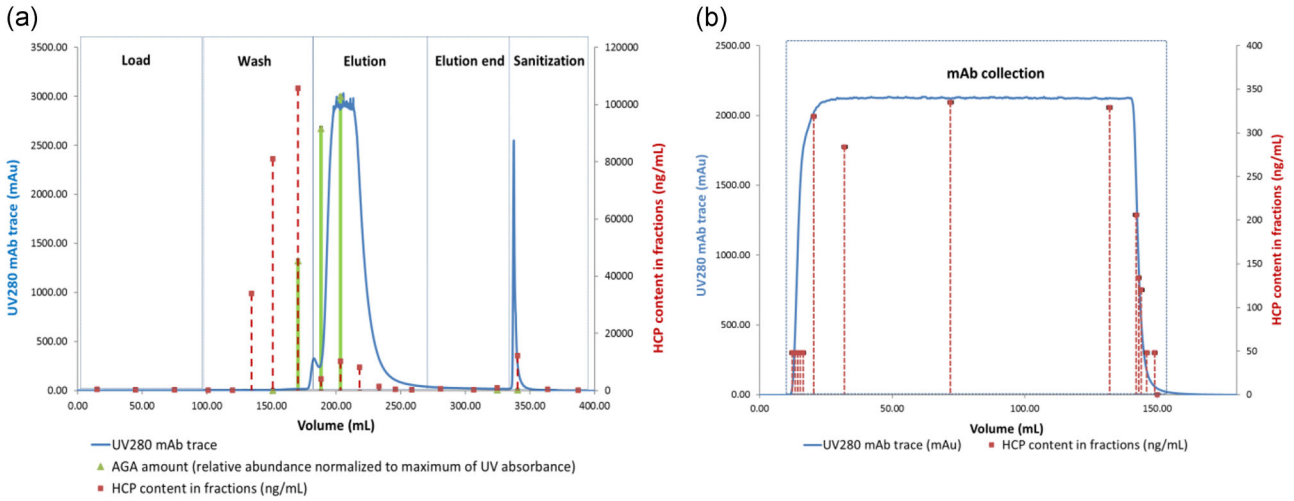

FIGURE 6 Fractionation studies for (a) first polishing step and (b) second polishing step. AGA, *N*-(4)-(β-acetylglucosaminyl)-L-asparaginase; HCP, host cell protein; mAb, monoclonal antibody [Color figure can be viewed at wileyonlinelibrary.com]

Fractions were also collected on the second polishing step (flow-through mode). As AGA was the only HCP identified post first polishing step, and, therefore, loaded on the column, only HCP quantitation by ELISA was performed. As previously observed for the first polishing step, AGA seems to follow the collected mAb1 profile (UV280; Figure 6b).

These studies have contributed to the understanding of HCP clearance during polishing steps that could be leveraged in further process optimization. Indeed, most HCP species were eliminated during the first polishing step wash phase while AGA copurifies with mAb1. The same behavior was observed in the second polishing step. Thus, both fractionation studies suggest an interaction of AGA with mAb1.

3.6 | More in-depth HCP profiling with native digestion protocol?

In 2017, a very elegant sample preparation method was published (Huang et al., 2017). It allowed a sharp increase in MS–HCP analysis dynamic range by removing a great majority of the mAb from the sample. This was achieved through tryptic digestion in native conditions followed by heat denaturation causing the precipitation of the undigested mAb. This preparation allowed a loaded sample increase on the column by 10 folds.

This method was applied to purification intermediates and DS on one batch before and one after HCP content increase. For comparison, samples were processed according to both preparation methods, denaturing, and native digestion protocols.

For both batches at the post capture step, while a maximum of nine HCP were identified with the denaturing digestion, up to 48 HCP including AGA were listed using the native digestion. However, for the second polishing step and for the DS, while AGA was identified in denaturing conditions, it was not detected in native ones. Moreover, no other HCP were identified on these steps that could explain the slight differences noted earlier between HCP ELISA and MS results.

Referring to the search engine scores (indicative of the relative abundance of a protein between different samples), at post capture step, in native conditions, every HCP was identified with a significantly higher score, except for AGA (Figure 7). This unexpected observation ($n = 3$) reinforce the hypothesis of a specific interaction between mAb1 and AGA that would compromise its digestion in native conditions and favor its coprecipitation. This result also

(a)

		Batch before HCP content increase				Batch after HCP content increase			
		Post capture step	Post 1st polishing step	Post 2nd polishing step	DS	Post capture step	Post 1st polishing step	Post 2nd polishing step	DS
Digestion in denaturing conditions	HCP number	6	1	1	0	9	1	1	1
	AGA identification	yes	yes	yes	no	yes	yes	yes	yes
Digestion in native conditions	HCP number	48	1	0	0	40	1	0	0
	AGA identification	yes	yes	no	no	yes	yes	no	no

(b)

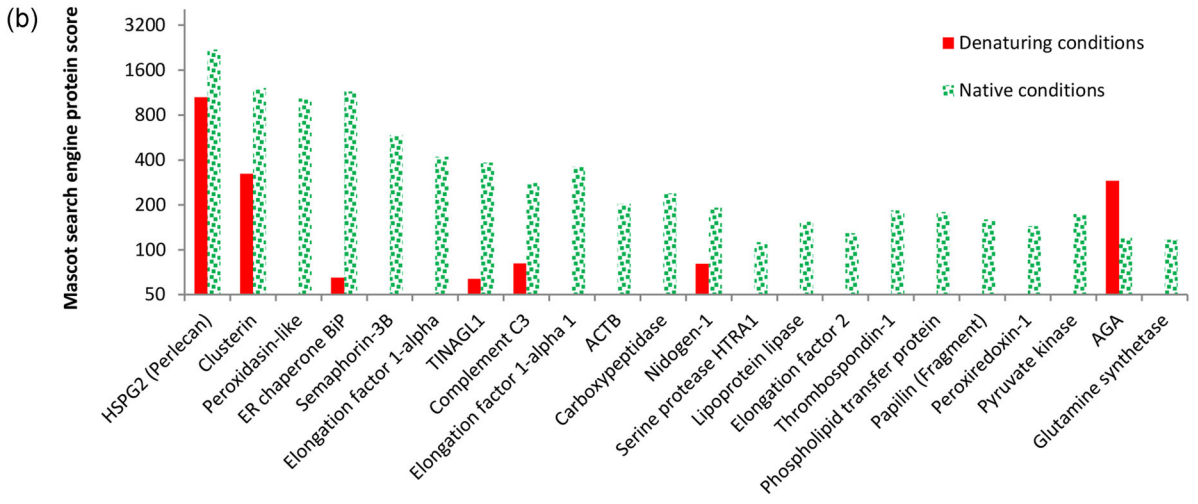

FIGURE 7 Comparison of HCP identification lists obtained by NanoLC–MS/MS using either mAb1 digestion in denaturing or in native conditions. (a) Numbers of HCP identified for each step and information on the presence or absence of AGA in the identification lists. (b) Mascot protein scores for the most abundant HCP identified in the post capture step for the two sample preparation protocols. AGA, *N*-(4)-(β-acetylglucosaminyl)-L-asparaginase; DS, drug substance; HCP, host cell protein; LC–MS, liquid chromatography–mass spectrometry [Color figure can be viewed at wileyonlinelibrary.com]

emphasizes the risk induced by sample preparation procedures aiming at enriching HCP by depleting the mAb as copurified HCP might be discarded even though they represent the greatest risk of residual HCP.

3.7 | AGA implication in potential protein–protein interaction

Several observations are described in Sections 3.5 and 3.6, let us speculate an interaction of AGA with mAb1. In a published cation exchange study, AGA was listed among the most abundant copurifying HCP (Joucla et al., 2013), indicating that AGA could either interact with the resins or with the mAb. LC–MS/MS results obtained here for the native digestion rather suggest an interaction with the mAb as the HCP is lost when the mAb is precipitated in the sample preparation. Following these observations, in silico surface analysis of AGA was performed to determine potential interaction zones with mAb1.

The homology model of AGA showed four exposed hydrophobic patches. The largest surface, in the template human structure, serves as a heterotetrametric-forming surface. We cannot exclude a priori the same behavior for the *Cricetulus griseus* ortholog showing the same surface (Figure S3a), but no indication so far pointing towards this hypothetical conformation was reported. Despite this potential interaction, three other hydrophobic patches can be observed on the surface of the homology model (Figure S3b–d). Moreover, either negatively or positively charged residues can be found within all these patches, suggesting a potential for protein–protein interaction. Eventually, the protein is rich in exposed histidine residues (Figure S3e), which are, in turn, very versatile side chains with respect to protein–protein interactions (Liao, Du, Meng, Pang, & Huang, 2013).

On the basis of aforementioned observations, we can speculate a strong potential for protein–protein interactions intrinsic to AGA. Further studies such as surface plasmon resonance and crosslinking MS could clarify this potential interaction but are beyond the scope of this paper.

4 | CONCLUSION

The case study presented herein demonstrates the importance of combining HCP quantitation by ELISA and MS tools for efficient analytical support to process development.

The use of HCP ELISA assay during IPM enabled to straightaway detect an increase in total HCP content. The additional observation of ELISA nonlinear dilution behavior has initiated an investigation. Thereafter, the deployment of MS tools led to the confirmation of ELISA results and to the identification of a single HCP, AGA. On the basis of identification of the HCP as AGA, a risk assessment was conducted and suggested a low probability of impact on product quality and patient safety. Production of recAGA protein was useful to test the limits of our analytical tools and to confirm that the so far used in-house ELISA remained the most suitable assay for total HCP quantitation. In addition, fractionation studies showed a copurification of AGA for both polishing steps, while loss of AGA identification with native digestion protocol suggested an interaction and a precipitation with mAb1. In silico characterization of AGA revealed several hydrophobic patches as well as histidine rich regions having a strong potential for protein–protein interaction. Finally, the knowledge gathered from both ELISA and MS on purification intermediates was used in the development of an optimized process allowing the disruption of the interaction of mAb1 with AGA and its elimination in the DS.

This study emphasizes the importance of a close collaboration between DSP and analytics at the early stages of process optimization associated with the implementation of an exhaustive analytical toolbox. Indeed, HCP ELISA assay dilutional linearity assessment combined with the key use of multiple MS approaches provides a good basis for efficient process-related impurities elimination. This optimized strategy is currently applied on all early-stage projects as a part of quality by design approach enhancing process robustness and DS quality with no delay to the lean-to-clinic challenge.

ACKNOWLEDGMENTS

The authors would like to thank Hélène Le Borgne for her contribution to recombinant *N*-(4)-(β-acetylglucosaminyl)-L-asparaginase characterization by mass spectrometry, Claire Borel, Ronan Crépin, Grégoire Bisch, Christophe Sourrouille, Véronique Chiche, and Caroline Chauchard for their contribution to the ad hoc stability study results generation, Emmanuel Berthelon, Frédérique David, Laura Borges, Thu-Quyen Nguyen, and Gwenaela Laignel for their contribution to host cell protein enzyme-linked immunosorbent assay results generation, Benoit Mothes and Claire Benac for their collaboration in the downstream process fractionation studies, and finally, Marc Ferron for his careful review of the manuscript and helpful suggestions.

CONFLICT OF INTERESTS

The authors declare that there are no conflict of interests.

ORCID

Séverine Clavier http://orcid.org/0000-0001-5938-2144
Shibani Mitra-Kaushik https://orcid.org/0000-0002-9119-0393
Yann Fromentin https://orcid.org/0000-0001-6049-0775

REFERENCES

Aronson, N. N., & Kuranda, M. J. (1989). Lysosomal degradation of Asn-linked glycoproteins. *FASEB Journal*, *3*(14), 2615–2622.

Bailey-Kellogg, C., Gutiérrez, A. H., Moise, L., Terry, F., Martin, W. D., & De Groot, A. S. (2014). CHOPPI: A web tool for the analysis of immunogenicity risk from host cell proteins in CHO-based protein production. *Biotechnology and Bioengineering*, *111*(11), 2170–2182. https://doi.org/10.1002/bit.25286

Bee, J. S., Tie, L., Johnson, D., Dimitrova, M. N., Jusino, K. C., & Afdahl, C. D. (2015). Trace levels of the CHO host cell protease cathepsin D caused particle formation in a monoclonal antibody product. *Biotechnology Progress*, *31*(5), 1360–1369. https://doi.org/10.1002/btpr.2150

Bracewell, D. G., Francis, R., & Smales, C. M. (2015). The future of host cell protein (HCP) identification during process development and manufacturing linked to a risk-based management for their control. *Biotechnology and Bioengineering*, *112*(9), 1727–1737. https://doi.org/10.1002/bit.25628

Chennamsetty, N., Voynov, V., Kayser, V., Helk, B., & Trout, B. L. (2010). Prediction of aggregation prone regions of therapeutic proteins. *The Journal of Physical Chemistry B*, *114*(19), 6614–6624. https://doi.org/10.1021/jp911706q

Dixit, N., Salamat-Miller, N., Salinas, P. A., Taylor, K. D., & Basu, S. K. (2016). Residual host cell protein promotes polysorbate 20 degradation in a sulfatase drug product leading to free fatty acid particles. *Journal of Pharmaceutical Sciences*, *105*(5), 1657–1666. https://doi.org/10.1016/j.xphs.2016.02.029

Gutiérrez, A. H., Moise, L., & Groot, A. S. D. (2012). Of [hamsters] and men. *Human Vaccines & Immunotherapeutics*, *8*(9), 1172–1174. https://doi.org/10.4161/hv.22378

Hall, T., Sandefur, S. L., Frye, C. C., Tuley, T. L., & Huang, L. (2016). Polysorbates 20 and 80 degradation by group XV lysosomal phospholipase A2 isomer X1 in monoclonal antibody formulations. *Journal of Pharmaceutical Sciences*, *105*(5), 1633–1642. https://doi.org/10.1016/j.xphs.2016.02.022

Huang, L., Wang, N., Mitchell, C. E., Brownlee, T., Maple, S. R., & De Felippis, M. R. (2017). A novel sample preparation for shotgun proteomics characterization of HCPs in antibodies. *Analytical Chemistry*, *89*(10), 5436–5444. https://doi.org/10.1021/acs.analchem.7b00304

Ikonen, E., Aula, P., Grön, K., Tollersrud, O., Halila, R., Manninen, T., … Peltonen, L. (1991). Spectrum of mutations in aspartylglucosaminuria. *Proceedings of the National Academy of Sciences of the United States of America*, *88*(24), 11222–11226.

Ikonen, E., Julkunen, I., Tollersrud, O. K., Kalkkinen, N., & Peltonen, L. (1993). Lysosomal aspartylglucosaminidase is processed to the active subunit complex in the endoplasmic reticulum. *The EMBO Journal*, *12*(1), 295–302.

Joucla, G., Le Sénéchal, C., Bégorre, M., Garbay, B., Santarelli, X., & Cabanne, C. (2013). Cation exchange versus multimodal cation exchange resins for antibody capture from CHO supernatants: Identification of contaminating host cell proteins by mass spectrometry. *Journal of Chromatography B, Analytical Technologies in the Biomedical and Life Sciences*, *942–943*, 126–133. https://doi.org/10.1016/j.jchromb.2013.10.033

Koterba, K. L., Borgschulte, T., & Laird, M. W. (2012). Thioredoxin 1 is responsible for antibody disulfide reduction in CHO cell culture. *Journal of Biotechnology*, *157*(1), 261–267. https://doi.org/10.1016/j.jbiotec.2011.11.009

Liao, S.-M., Du, Q.-S., Meng, J.-Z., Pang, Z.-W., & Huang, R.-B. (2013). The multiple roles of histidine in protein interactions. *Chemistry Central Journal*, *7*(1), 44. https://doi.org/10.1186/1752-153X-7-44

Makino, M., Kojima, T., & Yamashina, I. (1966). Enzymatic cleavage of glycopeptides. *Biochemical and Biophysical Research Communications*, *24*(6), 961–966. https://doi.org/10.1016/0006-291X(66)90344-5

McGovern, M. M., Aula, P., & Desnick, R. J. (1983). Purification and properties of human hepatic aspartylglucosaminidase. *The Journal of Biological Chemistry*, *258*(17), 10743–10747.

Oinonen, C., Tikkanen, R., Rouvinen, J., & Peltonen, L. (1995). Three-dimensional structure of human lysosomal aspartylglucosaminidase. *Nature Structural Biology*, *2*(12), 1102–1108. https://doi.org/10.1038/nsb1295-1102

Okazaki, A., Shoji-Hosaka, E., Nakamura, K., Wakitani, M., Uchida, K., Kakita, S., … Shitara, K. (2004). Fucose depletion from human IgG1 oligosaccharide enhances binding enthalpy and association rate between IgG1 and FcγRIIIa. *Journal of Molecular Biology*, *336*(5), 1239–1249. https://doi.org/10.1016/j.jmb.2004.01.007

Tikkanen, R., Riikonen, A., Oinonen, C., Rouvinen, R., & Peltonen, L. (1996). Functional analyses of active site residues of human lysosomal aspartylglucosaminidase: Implications for catalytic mechanism and autocatalytic activation. *The EMBO Journal*, *15*(12), 2954–2960. https://doi.org/10.1002/j.1460-2075.1996.tb00658.x

Vanderlaan, M., Zhu-Shimoni, J., Lin, S., Gunawan, F., Waerner, T., & Van Cott, K. E. (2018). Experience with host cell protein impurities in biopharmaceuticals. *Biotechnology Progress*, *34*(4), 828–837. https://doi.org/10.1002/btpr.2640

Wang, X., Hunter, A. K., & Mozier, N. M. (2009). Host cell proteins in biologics development: Identification, quantitation and risk assessment. *Biotechnology and Bioengineering*, *103*(3), 446–458. https://doi.org/10.1002/bit.22304

Zhu-Shimoni, J., Yu, C., Nishihara, J., Wong, R. M., Gunawan, F., Lin, M., … Vanderlaan, M. (2014). Host cell protein testing by ELISAs and the use of orthogonal methods. *Biotechnology and Bioengineering*, *111*(12), 2367–2379. https://doi.org/10.1002/bit.25327

SUPPORTING INFORMATION

Additional supporting information may be found online in the Supporting Information section.

How to cite this article: Clavier S, Fougeron D, Petrovic S, et al. Improving the analytical toolbox to investigate copurifying host cell proteins presence: *N*-(4)-(β-acetylglucosaminyl)-L-asparaginase case study. *Biotechnology and Bioengineering*. 2020;117:3368–3378. https://doi.org/10.1002/bit.27514